Comprehensive Journal of Science
Volume (10), Issue (37), (NOV. 2025)
SICST2025, www.sicst.ly
ISSN: 3014-6266

مجلة العلوم الشاملة
عدد خاص بالمؤتمر الدولي الثالث للعلوم والتقنية
المجلد (10)، العدد (37)، (نوفمبر2025)
ردمد: 3014-6266

# Fabrication and Performance evaluation of Cellulose Acetate Forward Osmosis Membrane (CAFSM) For Water Desalination

**Mohamed Farag Twibi [1*] , Saber Abdulhamid Alftessi[1] Husein D. Meshreghi [2], Abulkasim Faraj Ayad Alzerzah [1], Jamal Amar Ashour Eljourni[1]**

[1] Higher Institute of Science and Technology Soqalkhamis Imsehel, Tripoli, Libya
[2] Department, Faculty, University, City, Country
*Corresponding author: Dr.mohamedtwibi@gmail.com

# تصنيع وتقييم أداء غشاء التناضح الأمامي المصنوع من أسيتات السليلوز (CAFSM) لتحلية المياه

**محمد فرج الطويبي [1*] – صابر عبد الحميد الفطيسي [1] –حسين الضاوي المشرقي [2] – أبو القاسم فرج عياد الزرزاح [1] – جمال عمار عاشور الجورني [1]**

[1] المعهد العالي للعلوم والتقنية (سوق الخميس امسيحل) طرابلس /ليبيا
[2] كلية الطاقات المتجددة تاجوراء / ليبيا

Received: 9-11-2025; Revised: 15-11-2025; Accepted: 20-11-2025; Published: 25-11-2025

**Abstract:**

One of the greatest threats to human existence is the inability to cope with water supply demands. The forward osmosis (FO) process has therefore provided an alternative for the purification of water. The merit of utilizing FO is due to the fact that it works at low or no hydraulic pressure. In the current study, cellulose acetate flat sheet membranes (CAFSM) were fabricated using 20 wt.% CA, 48.33% acetone, and 31.66% formamide and tested for the FO process. The effect of evaporation time during casting was investigated. The evaporation times used in CAFSM are 0, 30, 60, and 90 seconds. The water flux of the CAFSM was measured using a 0.5M NaCl feed solution with different draw solutions of 2M NaCl and 2M $MgCl_2$.. The highest water flux achieved is 2.04 L/m²/h with the CAFSM prepared at 90 seconds evaporation time and using 2M NaCl draw solution. CAFSM prepared at 60 seconds evaporation time showed the lowest value of water flux of 0.288 L/m²/h. Heat treatment at 90°C improved the water flux of the CAFSM to 4.345 L/m²/h.

**Keywords:** Cellulose acetate flat sheet membranes (CAFSM); Forward osmosis (FO); Heat treatment.

**الملخص:**

يُعدّ عدم القدرة على تلبية احتياجات إمدادات المياه من أكبر التهديدات للوجود البشري. ولذلك، وفّرت عملية التناضح الأمامي (*FO*) بديلاً لتنقية المياه. تكمن ميزة استخدام *FO* في أنه يعمل عند ضغط هيدروليكي منخفض أو معدوم. في هذه الدراسة، صُنعت أغشية صفائحية مسطحة من أسيتات السليلوز (*CAFSM*) باستخدام 20% وزناً من أسيتات السليلوز، و48.33% أسيتون، و31.66% فورماميد، واختُبرت لعملية *FO*. ودُرست آثار زمن التبخر أثناء الصب. أزمنة التبخر المستخدمة في *CAFSM* هي 0، و30، و60، و90 ثانية. تم قياس تدفق الماء في *CAFSM* باستخدام محلول تغذية كلوريد الصوديوم بتركيز 0.5 مولار مع محاليل سحب مختلفة من كلوريد الصوديوم بتركيز 2 مولار وكلوريد المغنيسيوم بتركيز 2 مولار. وبلغ أعلى تدفق ماء 2.04 لتر/م²/ساعة باستخدام *CAFSM* المُحضر عند زمن تبخر 90 ثانية وباستخدام محلول سحب كلوريد الصوديوم بتركيز 2 مولار. وأظهر *CAFSM* المُحضر عند زمن تبخر 60 ثانية أقل قيمة لتدفق الماء، وهي 0.288 لتر/م²/ساعة. وقد حسّنت المعالجة الحرارية عند درجة حرارة 90 درجة مئوية تدفق الماء في *CAFSM* إلى 4.345 لتر/م²/ساعة.

**الكلمات المفتاحية:** أغشية أسيتات السليلوز المسطحة (CAFSM)، التناضح الأمامي (FO)، المعالجة الحرارية.

APHICAL ABSTRACT

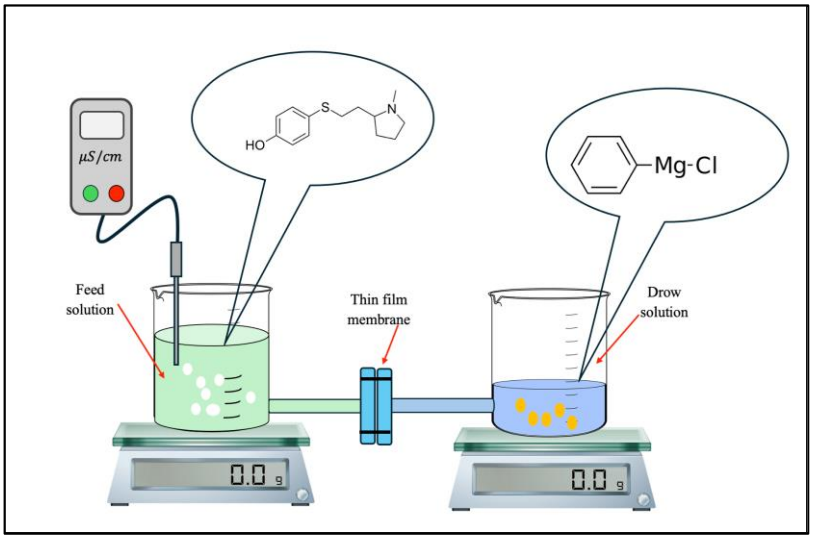

## INTRODUCTION

According to the World Health Organization, there are mainly three main categories of water sources for any township supply, and these include the rainwater, groundwater and surface water (Yeo & Seong, 2014a, 2014b). The ground water is the one obtained from dug wells, drilled wells, spring source, and subsurface wells. Water can be made accessible by damming a characteristic water catchment range, for example, a valley, and storing the water in the reservoir formed by the dam or occupying it to another reservoir. Important parameters in the planning of dams include the annual rainfall, the evaporation factor, water demand, and the geographical location of the area. One of the greatest threats to human existence is the inability to cope with water supply demands. Over 80% of used water worldwide is not collected or treated (Kookana et al., 2020). According to Biswas2014 (Biswas et al., 2024) the provision of improved sanitation and safe drinking water could reduce diarrhoeal diseases by nearly 90%. This is mostly experienced developing countries with lack of capacity to build the infrastructure required to mitigate the untoward impacts of these events.

The sporadic rise in the world population has greatly increased the demand for a clean water for household, agricultural and industrial purposes (Zhao, Zou, Tang, et al., 2012a). With about 2.6 billion of the world population in need of sufficient sanitized water, coupled with a projected 9-billion increment of the world population from the current 7 billion by 2050, the demand for clean water has also increased correspondingly (Carter, 2013). The population growth has therefore resulted to over one- third of the world's populace experiencing water shortage (Chung et al., 2012). The reality is that water management systems are not designed to meet all demands, given the full range of possible expected extreme events under what is understood to be contemporary hydrological variability (Seckler, 1998). The issue of clean water deficiency will be exasperated with this exponential populace growth. Therefore, a standout amongst the most urgent difficulties of the 21stcentury is to meet the expanding interest for clean water(Cath et al., 2006a; Chung et al., 2012). The generation of water is usually as arduous task requiring a large capital investment due

to the energy requirement (Ward & Pulido-Velazquez 2008). The forward osmosis process has therefore provided an alternative for power generation, purification of water, food concentration (Dova et al., 2007). The advantages of this method are its ability to maintain the colour and taste of the feed water without changing the quality of the water and this has placed it as a good source of water in drug production by pharmaceutical industries (Dova et al., 2007).

The major source of water in many parts of the world is saline or brackish water and this has greatly challenge research in water purification using affordable osmotic process. The forward osmosis therefore provides the alternative for desalinating and purifying the saline water due to the lower energy demand and cost of operation. This increase in demand for high quality water necessitated a need for a suitable flat sheet as membrane with lower hydraulic pressure, high osmotic power, and high rejection rate. The merit of utilizing forward osmosis (FO) is due to the fact that it works at low or no hydraulic pressure is required (Post et al., 2007). However, the only pressure experience during forward osmosis is the one due to the flow impedance in the semi permeable membrane.

This is opposed to the reversed osmosis (RO) which uses hydraulic pressure for water desalination(Anka & Balkus, 2013) In view of this prevailing challenges it is then necessary to design and fabricate a membrane for a forward osmosis process with ability for antifouling, low cost, low energy, high water flux and high recovery(Yeh et al., 2006).

## Experimental

### 1.1 Materials

Chemical used for making membrane which are cellulose acetate, acetone and formamide was purchased from Sigma, R&M chemical and Fisher scientific respectively. MgCl2 and NaCl

### 2.2 Preparation of Cellulose Acetate Flat Sheet Membrane(CAFSM)

As show in diagram 1 the CA powder was dried overnight at 75◦C in oven to remove the moisture. The spinning of dope solution was prepared by dissolving a certain

amount of Cellulose Acetate powders in the mixture of formamide and acetone at room temperature. The weight percentages of Cellulose Acetate, formamide and acetone in the dope solution were 20wt. %, 31.66wt.% and 48.33wt.% respectively. To avoid acetone evaporation, the mixing and dissolving were conducted in a 500mL blue-cap bottle sealed with para- film. The blue-cap bottle was mounted on a rotator and was rotated over night until a homogenous solution was obtained.

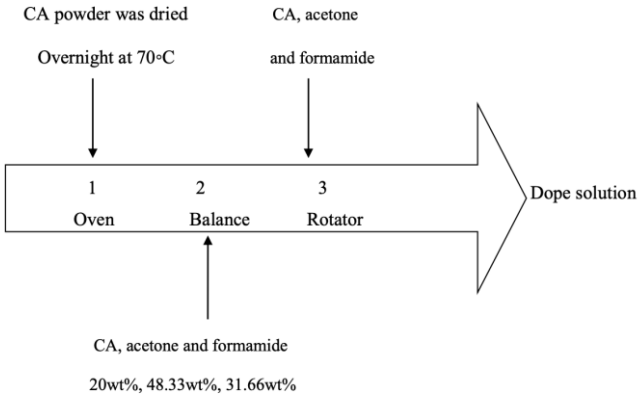


**Figure 1:** As show in diagram 1 dope solution preparations steps.

The preparation of flat sheet membranes begins by pouring the powder suspension into a reservoir behind the casting knife, followed by setting the carrier to be cast upon in motion. The thickness of the cast layer is determined by the casting knife gap between the carrier and the knife blade. Some of the other important variables are the reservoir depth, the carrier speed, and viscosity of the powder suspension. After casting, the wet cast layer is passed through the drying chamber to evaporate the solvent from the surface, leaving out a dry membrane precursor on the surface of the carrier. Normally, ceramic membranes that are prepared via tape casting have thickness in the range of a few millimeters (Zhu & Falls, 2008); however, the study by Shimizu *et al.* (Shimizu, 1990) prepared a $LaGaO_3$ solid electrolyte membrane and reported achieving 5μm thickness. Before start casting, we dope solution was put in ultrasonic one hour to remove bubbles. The cellulose acetate flat sheet membrane was fabricated through a

semi- automatic casting machine as shown in figure 2. Casting Speed was 3sec, and the evaporation time 0, 30, 60 and 90sec. 12.5g of dope solution was used to cast each flat sheet membrane. The conditions of casting were mentioned in table 1.

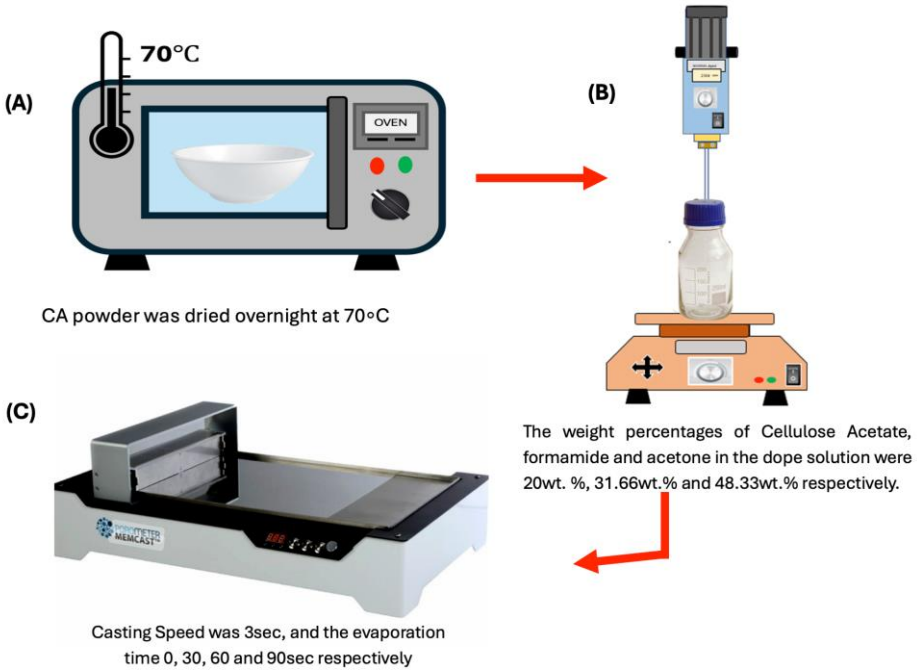


**Figure 2:** Schematic representation of the procedure applied to prepare the CA flat sheet membrane.

**Table 1** Casting conditions of the CA NF flat sheet membranes

| | |
|---|---|
| CA dope solution | CA/acetone/formamide (20:48.33:31.66) |
| Casting time (1) | 58.33 $sec^{-1}$ |
| Casting time (2) | 35,17.5and 11.66$sec^{-1}$ |
| Evaporation time | 0,30,60, and 90sec |
| Thickness of casting time | 200$\mu m$ |
| Dope solution temperature | 26°C |
| Room humidity | 65-70(%) |
| Coagulation bath | Tap water 26°C |

## 2.3 Heat-Treatment of The Ca Flat Fiber Membranes

The CAFSM after the phase inversion was divided into two groups as show in figure 3. The First group of membrane immersed in a water bath at 60◦C for 30min. Then

the water bath including the membranes cooled rapidly to room temperature by pouring cold water into the bath. The second group was heat-treated in two steps. After the same step of post-treatment, the fibers were transferred to a water bath at 95◦C for 30min, and then rapidly cooled by pouring cold water into the bath. both of the group of membrane were soaked in a 50wt.% glycerol aqueous solution for 48h and air-dried at room temperature before the membrane modules were made. After the flat sheet membrane has dried at room temperature, flat sheet was cut with length of 11.3cm and width of 5.5cm. Table 2 showed the detalis of cells.

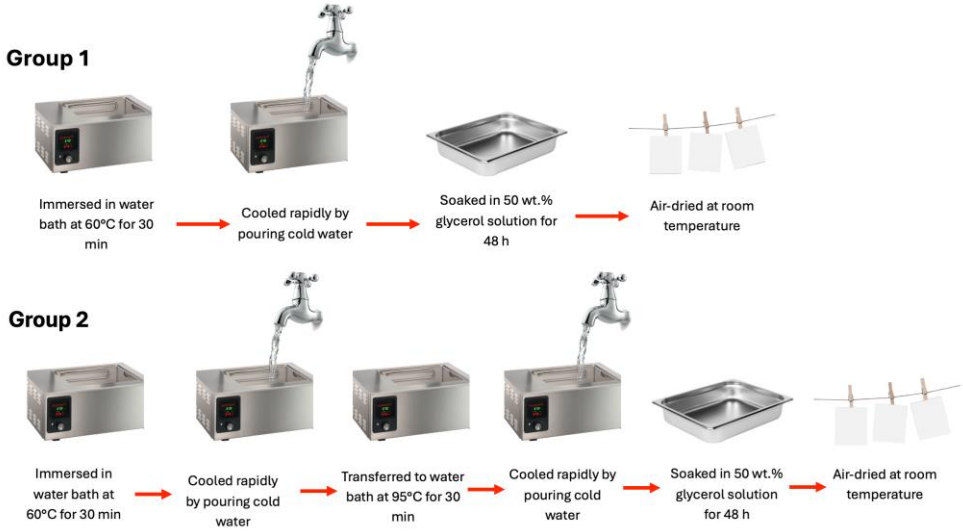


**Figure 3:** Heat-Treatment Of Cellulose Acetate Flat Sheet Membrane(CAFSM)

**Table 2 Details of Cells**

| | |
|---|---|
| Active Membrane Area | 42 $cm^2$ (6.5$in^2$) |
| Max Temperature | 80°C (180°F) |
| O-Ring | Buna-N |
| Outer Dimensions | 12.7× 10 × 8.3$cm$ (5 × 43.25 $in$) |
| Active Area Dimensions | 9.207× 4.572$cm$ (3.625 × 1.8$in$) |
| Slop Depth | 23cm (0.09in) |

## 2.4 Forward Osmosis Experimental Set-up

Feed solution was prepared by dissolving 58.4 g sodium chloride in 2L of DI water. The draw solution prepared by dissolving 203.3 g of MgCl2in 0.5 L of water. And

other draw solution prepared by dissolving 116.8g NaCl in 1L DI water, Feed and draw solution 200ml in reservoirs were placed on weighing balances and were circulated at a rate of 6.5±0.5 $L \cdot h^{-1}$ in a closed loop using gear pumps. All the experiments were conducted at 22°C. The area of the membrane used in the FO runs is 62.15$cm^2$ . The amount of water permeated over a period of time, flux ($L \cdot h^{-1} \cdot m^{-2}$) was measured from the change in the weight of draw solution during FO run. Water flux calculated by measuring the concentrations of NaCl in the draw solution and feed before and after FO runs by using the equation (1)

$$j_w = \frac{\Delta Volume}{Water\ denisty \times Mumbrane\ Surface\ Area \times Time} \qquad (1)$$

Where:

$j_w$ Water permeation flux.

$A$ Effective membrane area.

$\Delta V\ The$ weight of water permeated.

$\Delta t\ Predetermined\ time\ during\ thr\ FO\ tests.$

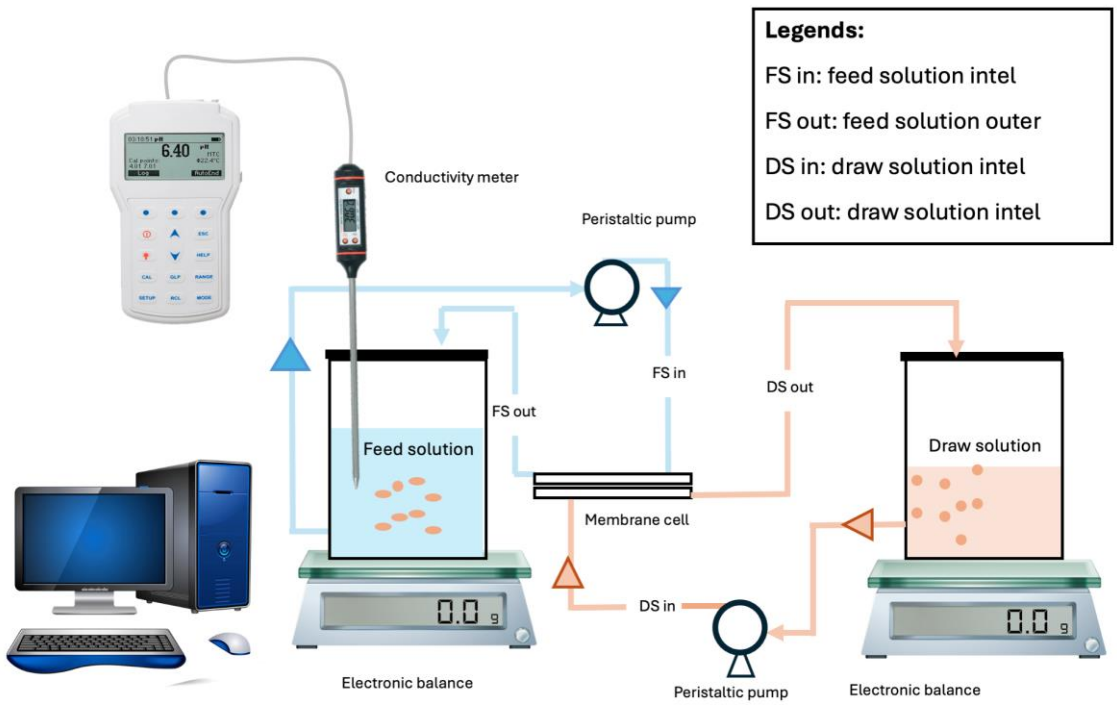


Figure 4: Set-up for FO system

**Performance tests in FO**

## 1.2 Effect of Evaporation Time on FO Performance

### 3.1.1 Effect of Evaporation Time on Water Flux

In terms of using NaCl as draw solution, the highest water flux combined with the highest evaporation time, was obtained with the CAFSM 90sec by 2.04 L/m$^2$.h, whereas the lowest point was recorded by 0.288 L/m$^2$.h with CAFSM 60sec, this may be due to the accumulation of salts near the membrane surface in draw solution side of the membrane. While there were slightly different between CAFSM 0sed, CAFSM 30sec by 0.925 and 0.784 L/m$^2$.h respectively. Regarding to MgCl2 as draw solution, the highest point of water flux was reached to the peak by 1.59 L/m$^2$.h with using CAFSM 90sec, while the lowest point was 0.936 L/m$^2$.h by using CAFSM 60sec. 1.07 and 0.936 L/m$^2$.h were obtained by using CAFSM 0sec and CAFSM 30sec respectively. In previous study done by (Gao et al., 2009)(Gao et al. 2009) investigated the effect of evaporation time on water flux, (PPO) was used as polymer in this study, the evaporation time used in range between 0 and 180 sec, when evaporation time increase, water flux of membrane continuously increase from the initial lower value of

169 L/$m^2$.h when evaporation time was 0 sec, while evaporation time increased to 30sec the water flux also increase to reached nearly 300L/$m^2$.h, after that the water flux increased slightly by 320L/$m^2$.h when the evaporation time was 60 sec, the water flux dramatically increased by 470L/$m^2$.h when evaporation time was 90sec.

In other previous study(Sairam et al., 2011) the polymer was used CA 6.4g. Membranes were casted with evaporation times 60 and 90 sec to explore the effect of evaporation time on flux at 60 sec of evaporation time was used to obtain result of water flux 6.4L/$m^2$.h and Permeability was 0.64L·$h^{-1}$·$m^{-2}$·$bar^{-1}$ while the evaporation time increased up to 90sec, water flux obtained by 6.1 L/$m^2$.h and the Permeability 0.6L·$h^{-1}$·m

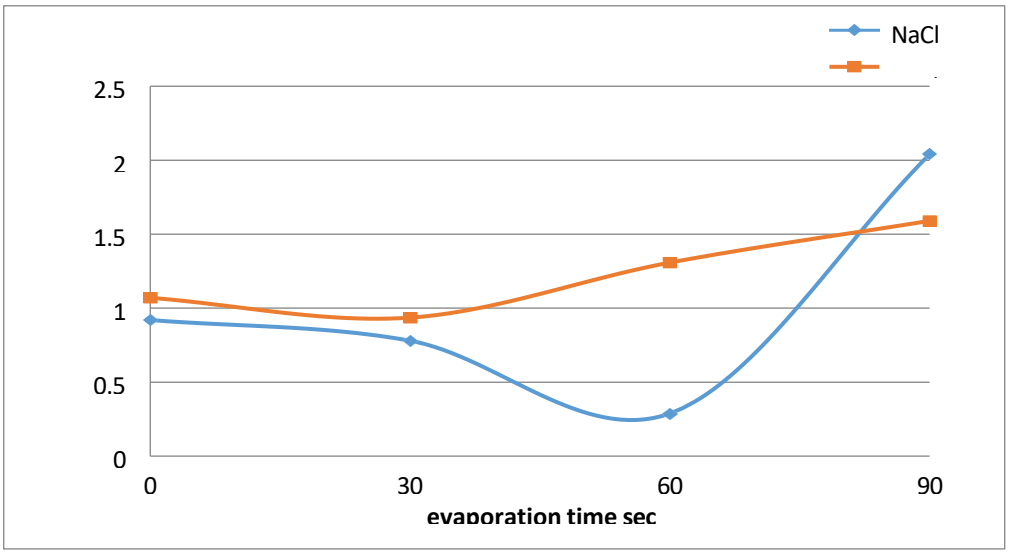


**Figure *5:*** Average of water flux against evaporation time NaCl and MgCl2 as draw solution

### 3.1.2 Effect Of Evaporation Time On Salt Flux

The performance of cellulose acetate (CA) membranes with different degrees of modification (CA#0, CA#30, CA#60, and CA#90) was assessed using water and salt flux across the feed and draw sides. As shown in Table 3. It is clearly to see that thein feed side CA#90 has the lowest salt flux 0.0174g/$m^2$.h However, an elevated draw-side salt flux (0.089 g/$m^2$·h) indicates possible structural or chemical alterations impacting selectivity. (Lee et al., 2011; Zhang et al., 2021), whereas the highest salt flux was

0.4361 g/m$^2$.h CA#60. In previous study done by (*Manjikian1967*, n.d.)(Cited et al. 1967) used cellulose acetate as polymer, the highest salt flux was 1.78g/l with 15 sec evaporation, salt flux decreased to 0.646g/l by used 30sec evaporation time, whereas salt flux was 0.578g/l with evaporation time 60sec. These changes underscore the influence of membrane modification on osmotic efficacy, indicating that intermediate modifications (CA#30, CA#60) may enhance salt rejection more effectively than either highly modified or unmodified membranes. Subsequent research should examine the trade-offs between water permeability and solute rejection in modified cellulose acetate membranes.

**Table 3 .Salt flux in feed and draw side with different evaporation time**

| membrane | Feed side | | | Draw side | | |
|---|---|---|---|---|---|---|
| | Before g/m$^2$.h | After g/m$^2$.h | salt flux g/m$^2$.h | Before g/m$^2$.h | After g/m$^2$.h | salt flux g/m$^2$.h |
| **CA#0** | 5.844 | 5.8621 | 0.0181 | 23.376 | 23.376 | 0.0 |
| **CA#30** | 5.844 | 5.569 | 0.2745 | 23.376 | 23.375 | 0.001 |
| **CA#60** | 5.844 | 5.4079 | 0.4361 | 23.376 | 23.369 | 0.0067 |
| **CA#90** | 5.844 | 5.826 | 0.0174` | 23.376 | 23.286 | 0.089 |

## 1.1 Effect of Casting Speed on FO Performance

### 1.1.3 Effect Casting Speed on Water Flux

Figure 3 illustrate the effect of casting time in water flux, and evaporation time 90sec. The highest water flux recorded by 4.435 L/m².h with 35sec casting time. Whereas casting time 17.5sec the water flux was decreased 1.565 L/m².h. The lowest water flux recorded 1.255 L/m².h by using 11.66sec casting time In recent study done by (Online et al. 2015) polymer was used polyethersulfone (PES), Casting shear rate 9.24, 23.51, and 42.67 sec, pure water flux were 25.13, 38.35 and 41.32L/m$^2$.h respectively. It can be seen that when casting time increase water flux continuously increase.

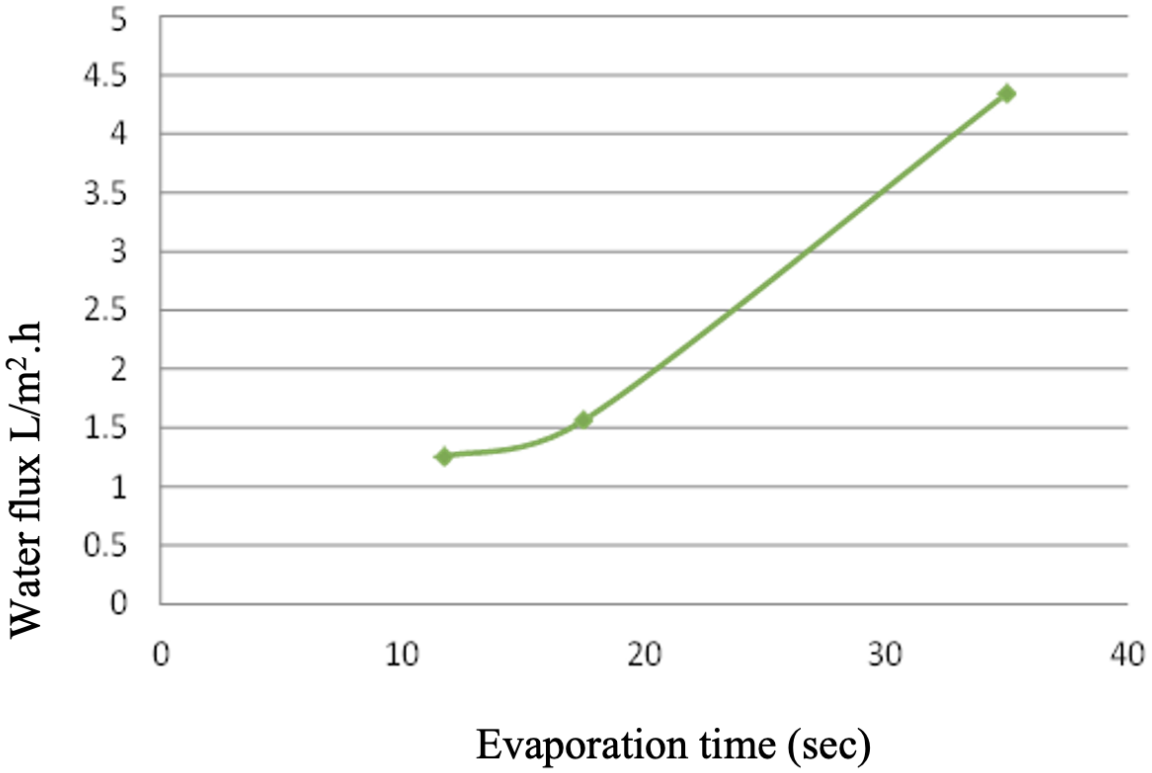


**Figure 3:** The effect of casting time in water flux, and evaporation time 90sec

### 1.1.4 Effect Of Casting Speed On Salt Flux

Table 4 presents the influence of casting speed on salt flux in a forward osmosis (FO) membrane system, as determined by mass differences before and after the process on both the feed and draw sides. At a high casting speed of 35 $s^{-1}$, minimal salt flux was observed—0.0009 g/m²·h on the feed side and 0.001 g/m²·h on the draw side—indicating limited reverse salt diffusion. When the casting speed was reduced to 17.5 $s^{-1}$, salt flux from the feed remained low (0.0001 g/m²·h), while the draw side showed an increased salt flux of 0.10 g/m²·h, suggesting elevated back-diffusion of solutes. At the lowest casting speed (11.66 $s^{-1}$), salt flux on the feed side rose significantly to 0.24 g/m²·h, while it remained stable at 0.001 g/m²·h on the draw side. These trends reflect the impact of casting speed on membrane microstructure—particularly skin layer thickness and porosity—which governs salt retention and diffusion properties (Sun et al., 2021)(Nair et al., 2019; Al-Juboori et al., 2021). Higher casting speeds typically yield thinner selective layers, reducing resistance to salt back-diffusion, while lower

speeds promote denser structures, which may either enhance or hinder salt flux depending on membrane integrity and internal concentration polarization (ICP) effects (Nawi et al., 2020; Shao et al., 2013a)(Tian et al., 2015; Heo et al., 2020). The increased salt flux at low casting speeds may be attributed to structural defects or increased internal diffusion pathways, emphasizing the need to optimize fabrication parameters for enhanced FO performance.

**Table 4.** The salt flux was obtained from using 2M NaCl as the draw solution and 0.5M NaCl as the feed with different evaporation time

| Casting speed ($Sec^{-1}$) | Feed side | | | Draw side | | |
|---|---|---|---|---|---|---|
| | Before $g/m^2.h$ | After $g/m^2.h$ | salt flux $g/m^2.h$ | Before $g/m^2.h$ | After $g/m^2.h$ | salt flux $g/m^2.h$ |
| **35** | 5.844 | 5.8439 | 0.0009 | 23.376 | 23.375 | 0.001 |
| **17.5** | 5.844 | 5.843 | 0.0001 | 23.376 | 23.270 | 0.10 |
| **11.66** | 5.844 | 5.602 | 0.24 | 23.376 | 23.375 | 0.001 |

### Effect Of Heat Treatment On FO Performance 1.1.5

As shown in figure 4 the relationship between evaporation time and heat treatment and the effect on the water flux. It was clearly to see that CAFSM 0sec with heat treatment 90°C the water flux reached to 0.92L/m2.h, whereas the water flux was 1.07 L/m2.h when heat treatment was 60°C. To move to the next column CAFSM 30sec, when heat treatment 60°C water flux was 0.361 L/m2.h, 90°C heat treatment water flux was 0.78 L/m2.h, The lowest water flux was 0.288 L/m2.h when heat treatment 90°C and CAFSM 3sec. The highest water flux recorded 2.04 L/m2.h when CAFSM 90sec and heat treatment 90°C, whilst the water flux was 1.32 L/m2.h when CAFSM 90sec was used with heat treatment 60°C.In previous used polyethersulfone ultrafiltration flat sheet membrane. Investigated the effect of heat treatment on the water flux. The effect

of heat treatment is clearly observed upon comparison of PES ultrafiltration membranes heated at 50, 100 and 150°C the untreated PES ultrafiltration membrane for pure water permeation 14.0 L/m$^2$.h pure water permeation. Whereas As heating temperature increased to 50°C the water flux was 12.5L/m$^2$.h. And when heat treatment increased to 100°C L/m$^2$.h, that is mean the heat treatment may have caused a reduction in pore size and the densification of the thin layer thus resulting in increased solute separation but lower flux. In other previous study (Cited et al. 1967) used CA as polymer, the evaporation time increased from 15 to 180 sec and the water flux decreased significantly from 142 to 42.666 L/m$^2$.h.

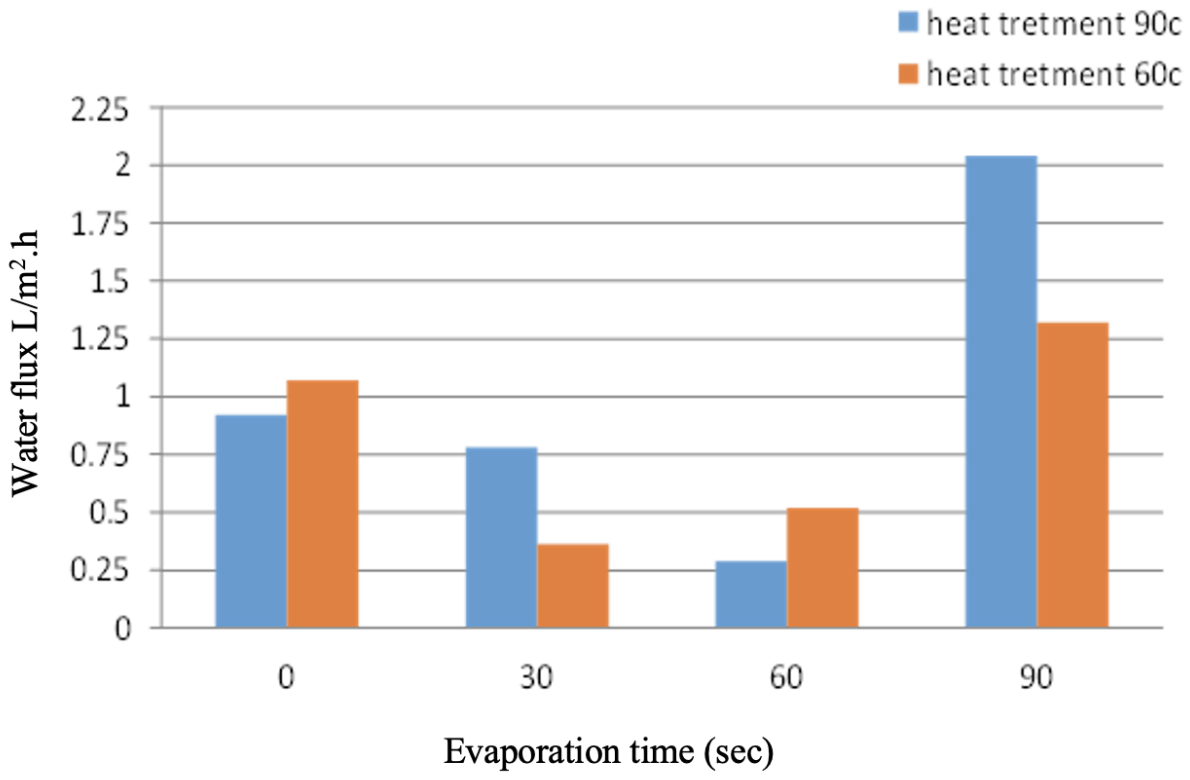


**Figure 4**: Effect of heat treatment and evaporation time in water flux

### 4.1 Effect of $Mgcl_2$ and Nacl AS Draw Solution On FO Preformance

As shown in Figure 4.4 the transportation of water across a semi-permeable membrane from a region of higher concentration to a region of lower concentration, the CAFSM 90 sec was used with two different draw solution MgCl2 and NaCl. As can be seen the volume of feed solution decrease when time increase, in first 10 min MgCl2 was used as draw solution the valium of feed solution decreased slightly 197.96 ml, in 20 min

the volume decrease sharply 193.79 ml, after that decreased gently to reach 193.02 ml, on the other hand NaCl was used as draw solution the result was slightly different, in first 10 min the valium of feed solution decreased sharply by 192.63 ml, after that every 10 min decreased slightly until reached to 189.46 ml and this was the highest volume got during this experiment.

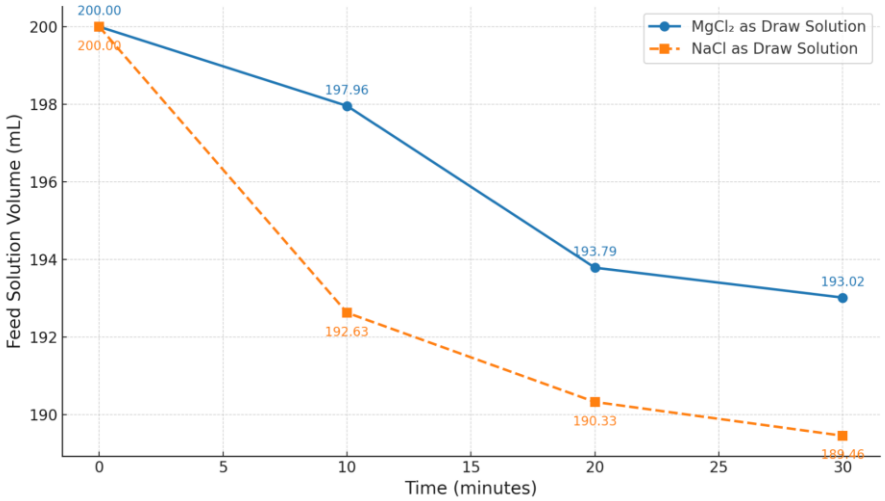


**Figure 5***:* Volume of feed solution against time use NaCl, MgCl2 as draw solution

Table 5 illustrates the variation in solute concentration and electrical conductivity on both the feed and draw solution sides during evaporation over a 90-second period. Initially, the feed solution had a concentration of 0.512 M and a conductivity of 48.18 mS, while the draw solution showed a higher concentration of 1.96 M and conductivity of 142.5 mS. As evaporation progressed, there was a slight decrease in feed concentration at 30 seconds (0.509 M), followed by a small increase at 60 seconds (0.524 M), and a marginal decline at 90 seconds (0.5226 M). The conductivity trend on the feed side mirrored these changes, fluctuating around 48–49 mS. In contrast, the draw solution exhibited a consistent decline in both concentration and conductivity, dropping to 1.74 M and 129.9 mS by 90 seconds. These changes suggest that water flux occurred from the feed to the draw solution due to osmotic pressure differences, with simultaneous evaporation affecting solute distribution and conductivity (Cath et

al., 2006b; Zhao, Zou, Tang, et al., 2012b). The slight fluctuations on the feed side may be attributed to the balance between osmotic back diffusion and water flux, as well as the effect of evaporative concentration at the interface (Achilli et al., 2009)(Achilli et al., 2009).

**Table 5** Concentration and conductivity in feed and draw side against Evaporation time

| vaporation time(sec) | Feed solution side | | Draw solution side | |
|---|---|---|---|---|
| | **Concentration M** | **Conductivity mS** | **Concentration M** | **Conductivity mS** |
| 0 | 0.512 | 48.18 | 1.96 | 142.5 |
| 30 | 0.509 | 47.92 | 1.88 | 139.21 |
| 60 | 0.524 | 49.31 | 1.79 | 133.62 |
| 90 | 0.5226 | 49.13 | 1.74 | 129.9 |

Table 6 presents the effect of casting speed on solute concentration and electrical conductivity in both the feed and draw solutions of a forward osmosis (FO) membrane system. As the casting speed decreased from 35 $s^{-1}$ to 11.66 $s^{-1}$, notable variations in concentration and conductivity were observed. At the highest casting speed (35 $s^{-1}$), the feed solution exhibited a concentration of 0.501 M and conductivity of 46.93 mS, while the draw solution showed a concentration of 1.92 M and conductivity of 142.1 mS. When the casting speed was reduced to 17.5 $s^{-1}$, the feed concentration increased to 0.52 M with a conductivity of 48.03 mS, and the draw solution concentration decreased slightly to 1.81 M with conductivity of 140.5 mS. Interestingly, at the lowest casting speed (11.66 $s^{-1}$), the feed concentration slightly decreased to 0.509 M, while the draw solution concentration rose again to 1.89 M; however, a sharp decline in draw conductivity to 41.05 mS was recorded. These fluctuations can be attributed to the influence of casting speed on membrane morphology, particularly pore structure and thickness, which directly affect water and solute transport properties (Achilli et al., 2009; Shao et al., 2013b). Faster casting speeds often lead to thinner membranes with higher permeability, whereas slower speeds may result in denser structures that alter

diffusion resistance and reverse salt flux (Cath et al., 2006b). The observed variations in conductivity also suggest changes in ionic mobility and membrane selectivity under different casting conditions.

**Table 6** Concentration and conductivity in feed and draw side against Casting time

| Casting speed ($sec^{-1}$) | Feed solution side | | Draw solution side | |
|---|---|---|---|---|
| | Concentration M | Conductivity mS | Concentration M | ıctivity mS |
| 35 | 0.501 | 46.93 | 1.92 | 142.1 |
| 17.5 | 0.52 | 48.03 | 1.81 | 140.5 |
| 11.66 | 0.509 | 47.1 | 1.89 | 41.05 |

Table 7 illustrates the variation in solute concentration and electrical conductivity in both feed and draw solution compartments over time during the forward osmosis (FO) process. At the initial stage (0 seconds), the feed solution had a concentration of 0.512 wt.% and a conductivity of 48.18 µS/cm, while the draw solution exhibited higher values of 1.96 wt.% and 142.5 µS/cm, respectively. As evaporation progressed, the feed side showed a slight increase in concentration and conductivity, reaching 0.524 wt.% and 49.31 µS/cm at 60 seconds. However, a mild decline was noticed at 90 seconds. Conversely, the draw side demonstrated a consistent decrease in both parameters, where concentration dropped to 1.74 wt.% and conductivity fell to 129.9 µS/cm after 90 seconds. These variations suggest a net water flux from the feed to the draw solution, diluting the latter while concentrating the former, consistent with osmotic-driven transport.Such trends align with the findings of Zhao et al [29], who reported similar reductions in draw solution conductivity due to dilution during FO experiments using NaCl and $MgCl_2$.

**Table 7** Concentration and conductivity in feed and draw said against Casting time

| Draw solution side | | | Feed solution side | |
|---|---|---|---|---|
| **ing time (sec)** | **Concentration** | **conductivity** | **Concentration** | **conductivity** |
| 5 | 0.501 | 46.93 | 1.92 | 142.1 |
| 10 | 0.52 | 48.03 | 1.81 | 140.5 |
| 15 | 0.509 | 47.1 | 1.89 | 41.05 |

## 5 CONCLUSION

CA based flat sheet membranes were fabricated and explored for FO applications. Heat-treatment at 90℃ for 20 min and the evaporation time 0,30,60,90 sec clearly affects in the water flux. The resultant flat sheet membrane has a highest water flux when NaCl used as draw solution CA#90, and lower salt flux in the NF tests. The CA flat sheet membrane heat-treated at 60℃ for 30min shows the efficiency in water flux less but in salt flux was very close with heat treatment 90℃. The effect on casting time. Membranes were cast with 35,17.5 and 11.66sec and evaporation times 90 sec to explore the effect of evaporation time on flux, when casting time decrease water flow increase and vice versa.

Reference

Achilli, A., Cath, T. Y., & Childress, A. E. (2009). Power generation with pressure retarded osmosis: An experimental and theoretical investigation. *Journal of Membrane Science*, *343*(1–2), 42–52. https://doi.org/10.1016/j.memsci.2009.07.006

Anka, F. H., & Balkus, K. J. (2013). Novel nanofiltration hollow fiber membrane produced via electrospinning. *Industrial and Engineering Chemistry Research*, *52*(9), 3473–3480. https://doi.org/10.1021/ie303173w

Biswas, S., Adhikary, M., Alam, A., Islam, N., & Roy, R. (2024). Disparities in access to water, sanitation, and hygiene (WASH) services and the status of SDG-6 implementation across districts and states in India. *Heliyon*, *10*(18), e37646. https://doi.org/https://doi.org/10.1016/j.heliyon.2024.e37646

Carter, N. T. (2013). Desalination and Membrane Technologies : Federal Research and Adoption Issues. *CRS Report for Congress*, 18.

Cath, T. Y., Childress, A. E., & Elimelech, M. (2006a). Forward osmosis: Principles, applications, and recent developments. *Journal of Membrane Science*, *281*(1), 70–87. https://doi.org/https://doi.org/10.1016/j.memsci.2006.05.048

Cath, T. Y., Childress, A. E., & Elimelech, M. (2006b). Forward osmosis: Principles, applications, and recent developments. In *Journal of Membrane Science* (Vol. 281, Issues 1–2, pp. 70–87). https://doi.org/10.1016/j.memsci.2006.05.048

Chung, T. S., Zhang, S., Wang, K. Y., Su, J., & Ling, M. M. (2012). Forward osmosis processes: Yesterday, today and tomorrow. *Desalination*, *287*, 78–81. https://doi.org/10.1016/j.desal.2010.12.019

Dova, M. I., Petrotos, K. B., & Lazarides, H. N. (2007). On the direct osmotic concentration of liquid foods. Part I: Impact of process parameters on process performance. *Journal of Food Engineering*, *78*(2), 422–430. https://doi.org/10.1016/j.jfoodeng.2005.10.010

*EFFECT OF HEAT TREATMENT ON THE PERFORMANCE AND STRUCTURAL DETAILS OF POLYETHERSULFONE ULTRAFILTRATION MEMBRANES*. (n.d.).

Gao, L., Tang, B., & Wu, P. (2009). An experimental investigation of evaporation time and the relative humidity on a novel positively charged ultrafiltration membrane via dry–wet phase inversion. *Journal of Membrane Science*, *326*(1), 168–177. https://doi.org/https://doi.org/10.1016/j.memsci.2008.09.048

Kookana, R. S., Drechsel, P., Jamwal, P., & Vanderzalm, J. (2020). Urbanisation and emerging economies: Issues and potential solutions for water and food security. *Science of The Total Environment*, *732*, 139057. https://doi.org/https://doi.org/10.1016/j.scitotenv.2020.139057

Lee, K. P., Arnot, T. C., & Mattia, D. (2011). A review of reverse osmosis membrane materials for desalination-Development to date and future potential. In *Journal of Membrane Science* (Vol. 370, Issues 1–2, pp. 1–22). https://doi.org/10.1016/j.memsci.2010.12.036

*manjikian1967*. (n.d.).

Nawi, N. I. M., Bilad, M. R., Anath, G., Nordin, N. A. H., Kurnia, J. C., Wibisono, Y., & Arahman, N. (2020). The water flux dynamic in a hybrid forward osmosis-membrane distillation for produced water treatment. *Membranes*, *10*(9), 1–13. https://doi.org/10.3390/membranes10090225

Post, J. W., Veerman, J., Hamelers, H. V. M., Euverink, G. J. W., Metz, S. J., Nymeijer, K., & Buisman, C. J. N. (2007). Salinity-gradient power: Evaluation of pressure-retarded osmosis and reverse electrodialysis. *Journal of Membrane Science*, *288*(1), 218–230. https://doi.org/https://doi.org/10.1016/j.memsci.2006.11.018

Sairam, M., Sereewatthanawut, E., Li, K., Bismarck, A., & Livingston, A. G. (2011). Method for the preparation of cellulose acetate flat sheet composite membranes for forward osmosis—Desalination using MgSO4 draw solution. *Desalination*, *273*(2), 299–307. https://doi.org/https://doi.org/10.1016/j.desal.2011.01.050

Seckler, D. William. (1998). *World water demand and supply, 1990 to 2025 : scenarios and issues*. International Water Management Institute.

Shao, J., Zhao, L., Chen, X., & He, Y. (2013a). Humic acid rejection and flux decline with negatively charged membranes of different spacer arm lengths and charge groups. *Journal of Membrane Science*, *435*, 38–45. https://doi.org/10.1016/j.memsci.2013.01.063

Shao, J., Zhao, L., Chen, X., & He, Y. (2013b). Humic acid rejection and flux decline with negatively charged membranes of different spacer arm lengths and charge groups. *Journal of Membrane Science*, *435*, 38–45. https://doi.org/10.1016/j.memsci.2013.01.063

Shimizu, Y. (1990). Ceramic membranes for bioprocesses. In *Membrane* (Vol. 15, Issue 4). https://doi.org/10.5360/membrane.15.179

Sun, L., Xu, K., Gui, X., Liu, L., Lin, Q., Song, X., & Wang, Z. (2021). Reduction–responsive sulfur–monoterpene polysulfides in microfiber for adsorption of aqueous heavy metal. *Journal of Water Process Engineering*, *43*. https://doi.org/10.1016/j.jwpe.2021.102247

Yeh, H. M., Cheng, T. W., & Tsai, J. W. (2006). Ultrafiltration on sizing agent solution in tubular-membrane module. *Chemical Engineering Communications*, *193*(6), 661–674. https://doi.org/10.1080/009864490515621

Yeo, R., & Seong, W. (2014a). *Charaterization of Draw Solution in Forward Osmosis Process for the Treatment of Synthetic River Water*. *January*.

Yeo, R., & Seong, W. (2014b). *Charaterization of Draw Solution in Forward Osmosis Process for the Treatment of Synthetic River Water*. *January*.

Zhang, H., Wang, X., Wang, L., Lv, Y., Zhang, Z., & Wang, H. (2021). Identifying the fouling behavior of forward osmosis membranes exposed to different inorganic components with high ionic strength. *Environmental Science and Pollution Research*, *28*(34), 46303–46318. https://doi.org/10.1007/s11356-021-14170-4

Zhao, S., Zou, L., & Mulcahy, D. (2012). Brackish water desalination by a hybrid forward osmosis-nanofiltration system using divalent draw solute. *Desalination*, *284*, 175–181. https://doi.org/10.1016/j.desal.2011.08.053

Zhao, S., Zou, L., Tang, C. Y., & Mulcahy, D. (2012a). Recent developments in forward osmosis: Opportunities and challenges. In *Journal of Membrane Science* (Vol. 396, pp. 1–21). https://doi.org/10.1016/j.memsci.2011.12.023

Zhao, S., Zou, L., Tang, C. Y., & Mulcahy, D. (2012b). Recent developments in forward osmosis: Opportunities and challenges. In *Journal of Membrane Science* (Vol. 396, pp. 1–21). https://doi.org/10.1016/j.memsci.2011.12.023

Zhu, P., & Falls, I. (2008). *Ceramic Membranes for Permeation*.